Available online at www.sciencedirect.com
ScienceDirect
Journal of the European Ceramic Society 31 (2011) 825–831
www.elsevier.com/locate/jeurceramsoc

Factors that influence the flexural strength of SiC-based porous ceramics used for hot gas filter support

Junfeng Li [a], Hong Lin [a,*], Jianbao Li [a,b]

[a] State Key Laboratory of New Ceramics & Fine Processing, Department of Materials Science and Engineering, Tsinghua University, Beijing 100084, China
[b] Key Laboratory for Hainan Advantage Resources and Applied Technology in Chemical Engineering Material of Ministry of Education, Hainan Provincial Key Laboratory of Research on Utilization of Si–Zr–Ti, Materials and Chemical Engineering Institute, Hainan University, Haikou 570228, China

Received 9 August 2010; received in revised form 15 November 2010; accepted 28 November 2010
Available online 18 December 2010

Abstract

The influences of molding pressures, bonding phase contents, and SiC particle sizes on the flexural strength of SiC-based porous ceramics were investigated based on their microstructure of fracture surface. The SEM morphologies and EDS element analysis results of fracture surface showed that there were two different kinds of fracture points: SiC particle fracture points and bonding phase fracture points. It is found that molding pressures, bonding phase contents, and SiC particle sizes affect the SiC particle fracture point area in the fracture surface, and the fraction of the SiC particle fracture point area in the minimum solid area of fracture surface is a determined influence factor for the flexural strength of SiC-based porous ceramics used for hot gas filter support.

Keywords: Sintering; Porosity; Fracture; SiC; Structural applications

1. Introduction

Hot gas particulate ceramic filter is widely used in advanced coal-based power generation systems such as pressurized fluidized-bed combustion (PFBC) and integrated gasification combined cycle (IGCC).[1–3]

Silicon carbide (SiC) ceramic, which has high temperature stability, low thermal expansion coefficient, high corrosion resistance, high thermal conductivity and excellent mechanical properties, is suitable material as porous ceramic supports for hot gas cleaning.[4–8] However, it is difficult to sinter pure SiC ceramics below 2100 °C due to its strong covalent nature.[9] One effective way of fabricating porous SiC ceramics at low temperatures is to add a small amount of bonding phases to bond SiC particles together. Several researchers have done such work. Ohji and coworkers added a little alumina to SiC powder and fabricated porous SiC ceramics by an oxidation-bonding process, and investigated the flexural strength and thermal shock behavior of the porous SiC ceramics.[10–12] Jiang et al. prepared mullite-bonded and cordierite-bonded SiC porous ceramics, and investigated the effects of sintering temperatures and molding pressures on the flexural strength and porosity of the porous ceramics.[13–17]

The flexural strength of bonding phases, such as mullite, cordierite, and glass, is different from that of SiC particle skeletal phase, and generally lower. However, previous studies ignored to consider how SiC particle skeletal phase and bonding phase separately affected the flexural strength of SiC-based porous ceramics.

According to the minimum solid area models by Rice,[18–20] the strength–porosity dependence can be approximated as follows:

$$\sigma = \sigma_0 \exp(-bP) \quad (1)$$

Here, σ is the flexural strength of porous structure, σ_0 is the flexural strength of corresponding nonporous structure at the same composition, P is the porosity of porous structure, and b is a parameter determined by pore characteristics. When porous ceramics are formed by particles stacking, b mainly depends on the particle stacking types. When the values of b are 9 and 5 for solid spheres in rhombic stacking and cubic stacking, the particle coordination numbers are 12 and 6, corresponding to a tight

* Corresponding author. Tel.: +86 10 62772672; fax: +86 10 62772672.
E-mail address: hong-lin@tsinghua.edu.cn (H. Lin).

0955-2219/$ – see front matter © 2010 Elsevier Ltd. All rights reserved.
doi:10.1016/j.jeurceramsoc.2010.11.033

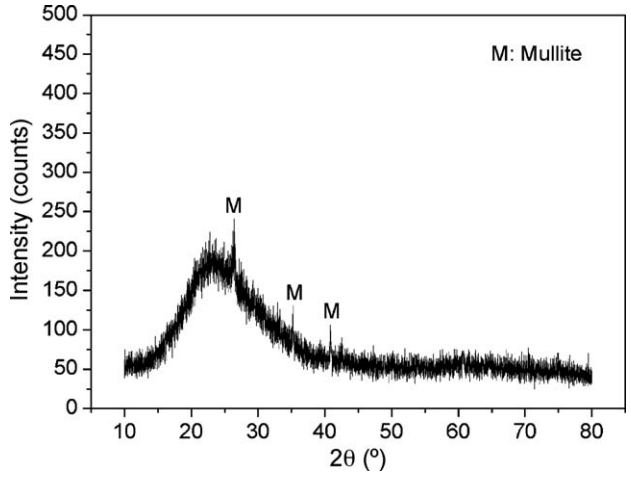

Fig. 1. XRD pattern of bonding phase (12 wt% kaolinite, 65 wt% potassium feldspar, and 23 wt% silica) sintered at 1300 °C for 3 h.

stacking and a loose stacking, respectively. The flexural strength is primarily determined by the minimum solid area fraction of the fracture surface when the other aspects of porous ceramics, such as the composition and the pore characteristics that may affect the flexural strength of porous ceramics, are not dominant. The minimum solid area for SiC-based porous ceramics formed by stacking SiC particles is the whole cumulative area of all fracture points on the fracture surface.

The purpose of this paper is to investigate how molding pressures, bonding phase contents, and SiC particle sizes affect the flexural strength of SiC-based porous ceramics. In addition, the influence of the microstructure of SiC-based porous ceramics on their flexural strength was discussed in detail.

2. Experimental procedure

The volume average diameters of SiC particles used in the experiment were 87 μm, 123 μm, 239 μm, and 300 μm, measured by a laser particle size analyzer (Model mastor 2000, Malvern Instruments Ltd., British). The bonding phase was a mixture of kaolinite (12 wt%), potassium feldspar (65 wt%), silica (23 wt%), which were mixed together by ball milling for 36 h. Four groups of samples, which will be referred to as M10, M15, B15, and P87, were prepared and each group included four samples. The samples of the group M10 contained 10 wt% bonding phase, the samples of the group M15 contained 15 wt% bonding phase, the bonding phase contents of the samples of the group B15 changed from 15 wt% to 25 wt%, and the SiC particle sizes of the samples of the group P87 changed from 87 μm to 300 μm. The SiC particles and bonding phase were homogeneously mixed together firstly by ball milling, and then extra 6 wt% graphite was added as a pore former. The mixed powder was uniaxially pressed into disks with 50 mm diameter and about 10 mm thickness at different pressures (6–91 MPa), and these samples were sintered at 1300 °C for 3 h at a heating rate of 5 °C/min. The sintered disks were machined into the rectangular specimens with dimensions of ~5 mm × 6 mm × 36 mm, and five such specimens for each sample were tested to obtain an average flexural strength.

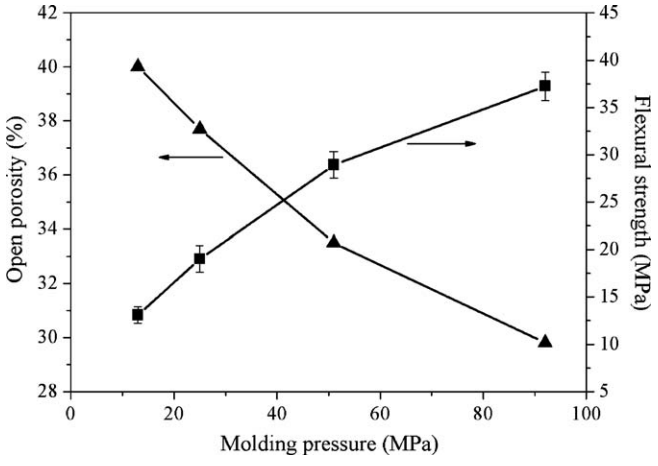

Fig. 2. Changes of porosity and flexural strength versus the molding pressure for the group M10 containing 10 wt% bonding phase.

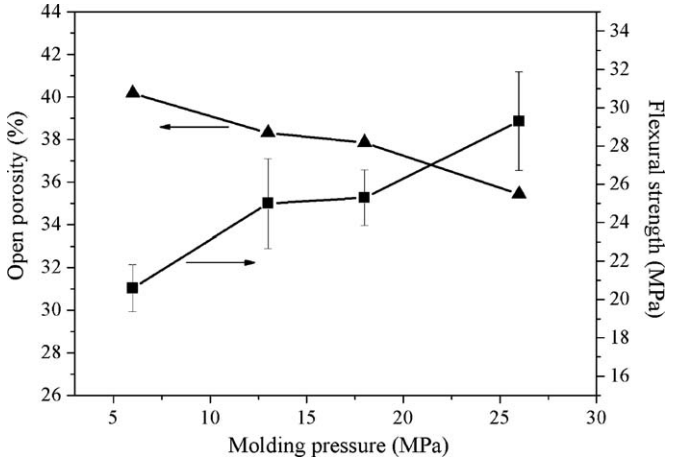

Fig. 3. Changes of porosity and flexural strength versus the molding pressure for the group M15 containing 15 wt% bonding phase.

Open porosity was determined by the Achimedes method using distilled water as the immersion medium. Flexural strengths were characterized via the three-point bending test (Model EHF-10L, Shimadzu, Japan) with a support distance of 30 mm, and a cross-head speed of 0.5 mm/min. The phase composition of bonding phase heated at 1300 °C was identified using an X-ray diffractometer (XRD; D/max-2550, Rigaku, Japan), operated at 200 kV, 45 mA, with experimental conditions as follows: a step width 0.02° and a scanning range of 10–80°. Fracture morphologies of porous specimens were observed by a scanning electron microscopy (SEM; SS-550, Shimadzu, Japan). The fracture point composition of porous specimens was measured by Energy Dispersive X-ray Spectroscopy (EDS) attached in the SEM instrument.

3. Results and discussion

Fig. 1 shows the XRD pattern of bonding phase sintered at 1300 °C, which indicated that the bonding phase, initially composed of kaolinite, feldspar, and silica, became a glassy phase with a small amount of mullite after being sintered. A glassy

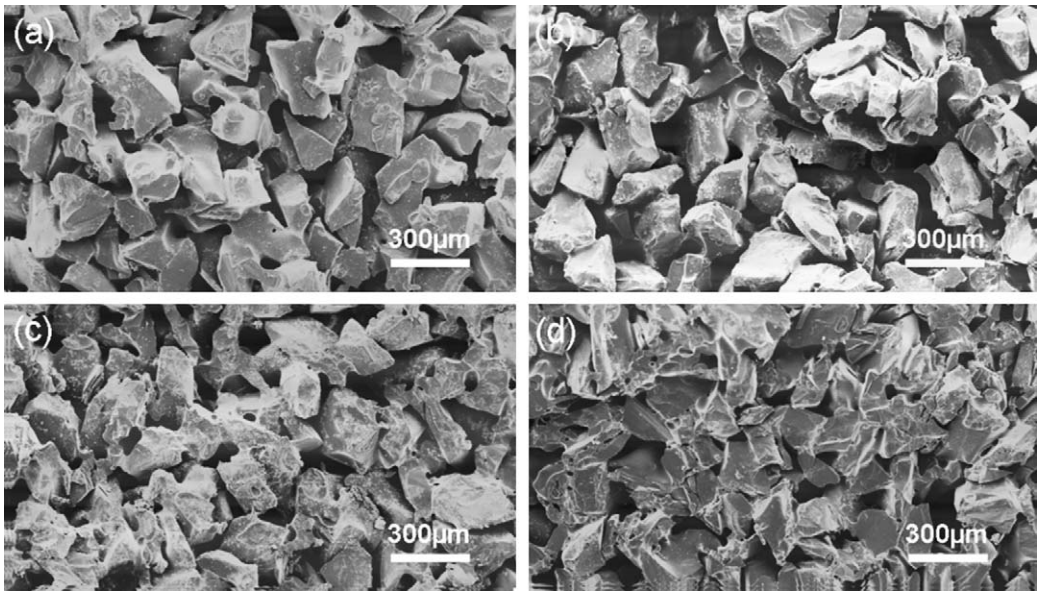

Fig. 4. Fracture surface morphologies of the group M10 containing 10 wt% bonding phase.

bonding phase was beneficial to forming SiC-based porous ceramics with homogeneous structure.

The porosity and flexural strength of SiC-based porous ceramics formed at different molding pressures are shown in Figs. 2 and 3. The four samples of the group M10 in Fig. 2, which contained 10 wt% bonding phase, were compressed into the green bodies at 13 MPa, 26 MPa, 51 MPa, and 91 MPa. The four samples of the group M15 in Fig. 3, which contained 15 wt% bonding phase, were compressed into the green bodies at 6 MPa, 13 MPa, 18 MPa, and 26 MPa. The porosity of SiC-based porous ceramics in Figs. 2 and 3 decreased with increasing the molding pressures, while the flexural strength of SiC-based porous ceramics correspondingly increased. The trend of the flexural strength change versus the porosity is consistent with the relationship in Eq. (1), and the porosity affected the flexural strength of SiC-based porous ceramics by changing the minimum solid area of fracture surface that increased with decreasing the porosity of SiC-based porous ceramics.[18] The fracture surface morphologies of the group M10 and the group M15 are shown in Figs. 4 and 5. It shows that the glassy bonding phase was homogeneously distributed on the SiC particle surface, which suggested a homogeneous porous structure was

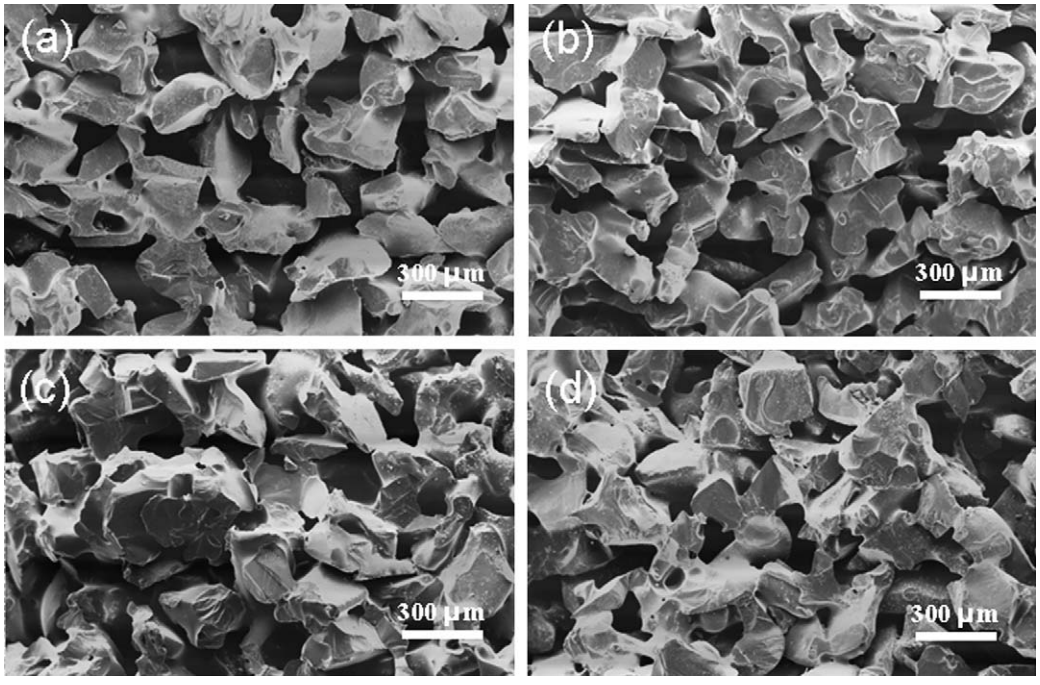

Fig. 5. Fracture surface morphologies of the group M15 containing 15 wt% bonding phase.

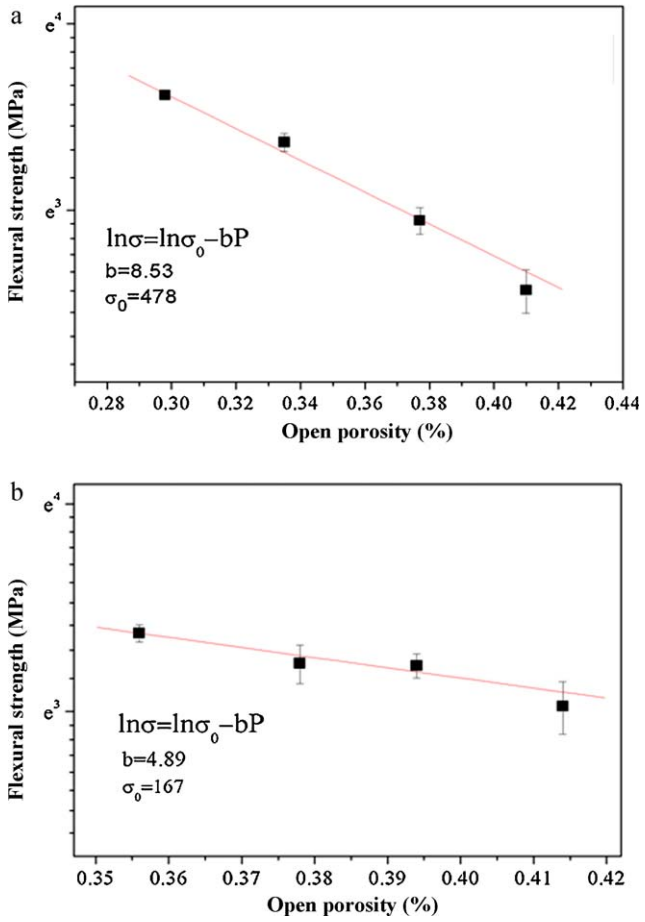

Fig. 6. Flexural strength as a function of porosity for the group M10 containing 10 wt% bonding phase (a) and the group M15 containing 15 wt% bonding phase (b).

formed, and the whole fracture point area (minimum solid area) increased with increasing the flexural strength in Figs. 4 and 5. Chae et al. also found that the homogenous microstructure of porous ceramics is conductive to a strength increase of porous ceramics.[21]

The relationships of the porosity to the flexural strength in Figs. 2 and 3 were well fitted by Eq. (1), as shown in Fig. 6a and b. The results suggested that the flexural strength was mainly determined by the minimum solid area fraction of the fracture surface when the composition of SiC-based porous ceramics was constant. The flexural strengths of the composite composed of SiC and bonding phase without porosity, σ_0, were obtained as 478 MPa for the group M10 and 167 MPa for the group M15, which showed that the values of σ_0 had a large decrease when bonding phase contents increased from 10 wt% to 15 wt%.

The fracture-point morphologies of SiC-based porous ceramics are shown in Fig. 7, in which there were two kinds of fracture points. One was the bonding phase fracture point, as shown in the folded part enclosed by the ellipse in Fig. 7b, and its element composition was shown in Fig. 7a. The other one was the SiC particle fracture point, as shown in the smooth part enclosed by the pane in Fig. 7b, and its element composition was shown in Fig. 7c. Comparing the element intensities in Fig. 7a with that in Fig. 7c, it is found that the ratios of the element intensities of Si and C were close to 3 in Fig. 7a, and approximately 1 in Fig. 7c. Meanwhile, there was more O element in Fig. 7a than Fig. 7c, and all above results supported that the division on the fracture-point types was reasonable.

The large decrease in σ_0 from the group M10 to the group M15 was attributed to that the SiC particle stacking types in the SiC-based porous ceramics approximately changed from rhombic type to cubic type. Moreover, the changes of SiC particle stacking types from rhombic type to cubic type reduced the fraction of the SiC particle fracture point area in the minimum solid area of fracture surface. The SiC particle stacking types in SiC-based porous ceramics can be obtained from the values of b by fitting the data of porosity and corresponding flexural strength according to equation 1 (Fig. 6). The values of b for the group

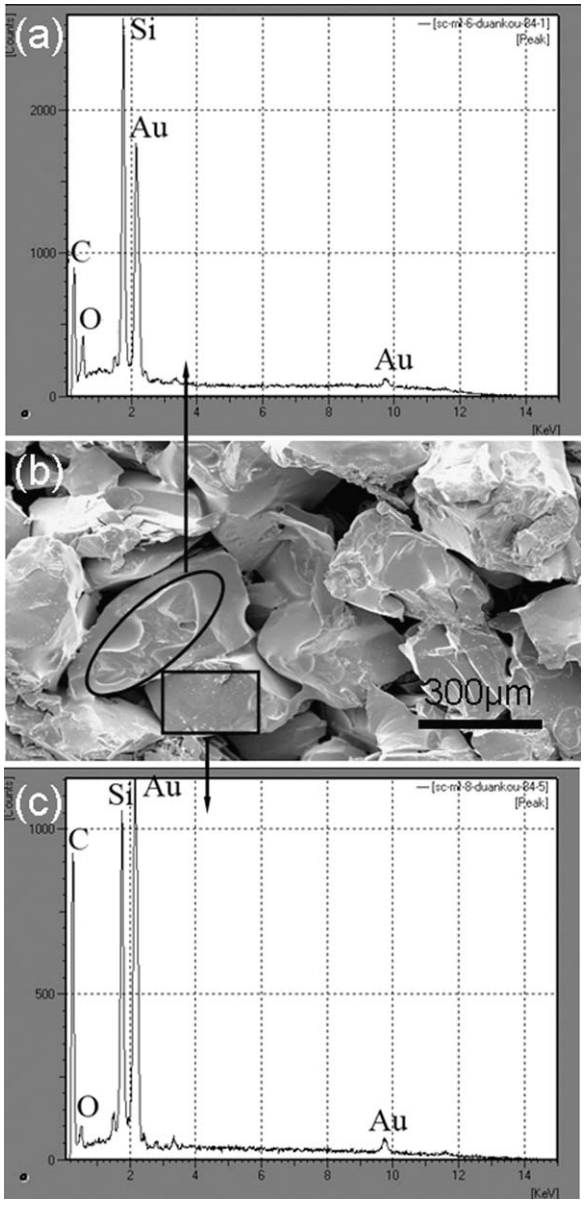

Fig. 7. Two different kinds of fracture points on the fracture surface (a) the elements composition of bonding phase fracture point, (b) the morphologies of bonding phase fracture point and SiC particle fracture point, and (c) the elements composition of SiC particle fracture point.

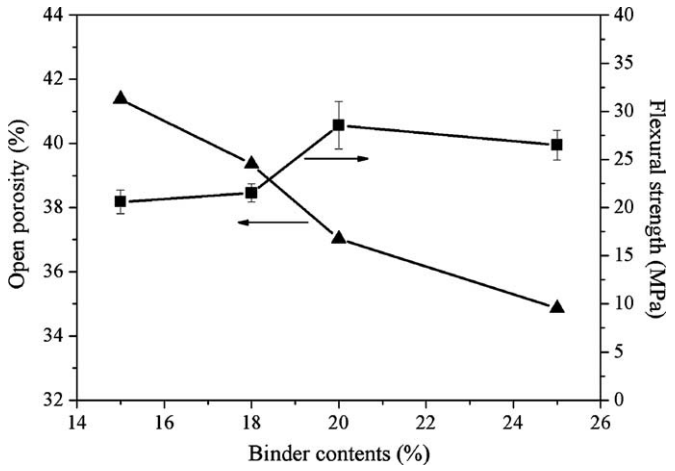

Fig. 8. Changes of porosity and flexural strength versus the bonding phase contents in the group B15 formed at a fixed molding pressure of 6 MPa.

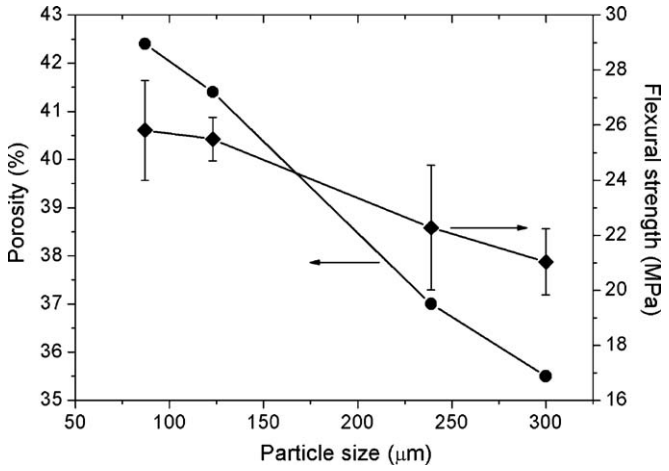

Fig. 10. Changes of porosity and flexural strength versus the SiC particle size in the group P87 with bonding phase of 20 wt% and molding pressure of 6 MPa, (a) 87 μm, (b) 123 μm, (c) 239 μm, and (d) 300 μm.

M10 and the group M15 were 8.53 and 4.89, respectively, which were close to 9 and 5 and suggested that the particle stacking types were close to rhombic type and cubic type.[18] Above all, the flexural strength of the composite composed of SiC and bonding phase without porosity, σ_0, depends on not only the composition of SiC-based porous ceramics but also the fraction of the SiC particle fracture point area in the minimum solid area of fracture surface.

Fig. 8 shows the effects of bonding phase contents on porosity and corresponding flexural strength of SiC-based porous ceramics. The four samples in Fig. 8 were all formed at 6 MPa and contained 15 wt%, 18 wt%, 20 wt%, and 25 wt% bonding phase, respectively. The porosity of the four samples decreased with increasing the bonding phase contents from 15 wt% to 25 wt%, having a similar changing tendency as that with increasing the molding pressures, while the flexural strength of the four samples firstly increased with increasing the bonding phase content to 20 wt%, followed by a decrease with further increasing the bonding phase content to 25 wt%. The morphologies of SiC-based porous ceramics containing different bonding phase contents are shown in Fig. 9. More SiC particle fracture points were included in the sample with 20 wt% bonding phase (Fig. 9c), and much more bonding phase fracture points were included in the sample with 25 wt% bonding phase (Fig. 9d), all of which supported that the two kinds of fracture points definitely existed in the SiC-based porous ceramics.

This variation of the flexural strength with increasing the porosity in Fig. 8 is inconsistent with the relationship given by Eq. (1), and the flexural strength of the sample containing 25 wt% bonding phase should have been higher than that of the sample containing 20 wt% bonding phase, because the former had lower porosity. The samples in Fig. 8 were formed at the

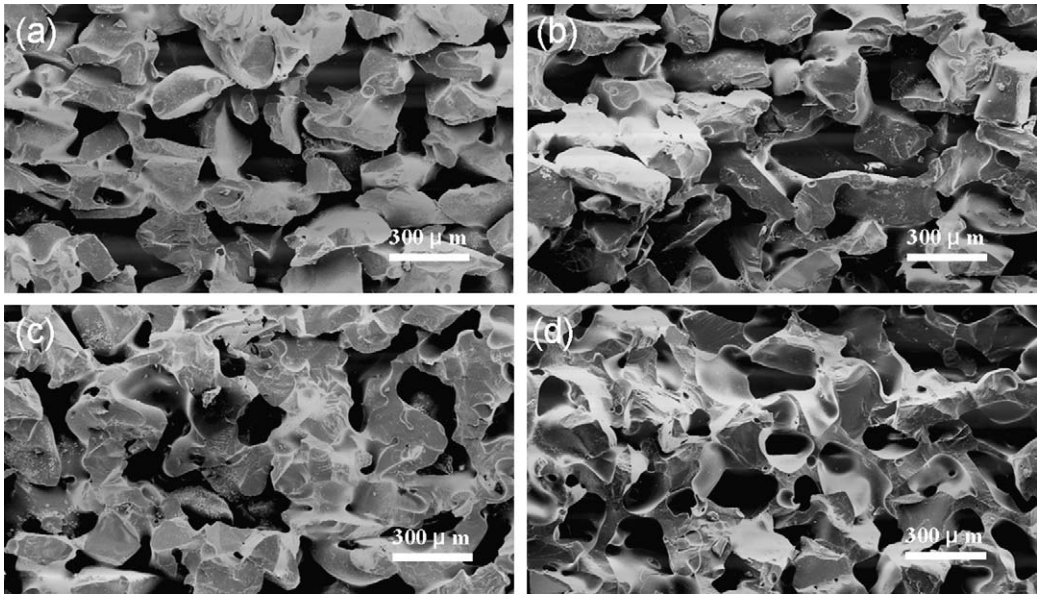

Fig. 9. Morphologies of the samples in the group B15 containing different bonding phase contents, (a) 15 wt%, (b) 18 wt%, (c) 20 wt%, and (d) 25 wt%.

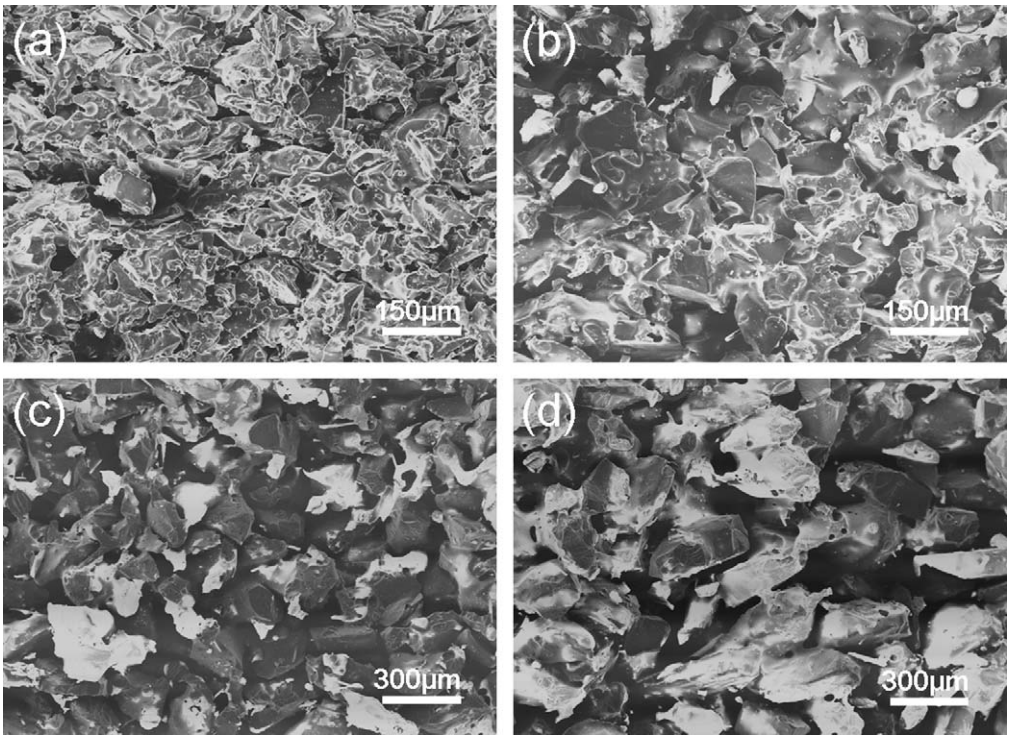

Fig. 11. Morphologies of the samples with different SiC particle sizes in the group P87 with bonding phase of 20 wt% and molding pressure of 6 MPa, (a) 87 μm, (b) 123 μm (c) 239 μm, and (d) 300 μm.

same molding pressure, and thus their SiC particle stacking types were similar. Therefore, the phenomenon was mainly attributed to that the fraction of the SiC particle fracture point area in the minimum solid area of fracture surface first increased and then decreased with increasing the bonding phase contents, which can be indirectly verified by that there were more smooth SiC particle fracture points in the sample containing 20 wt% bonding phase (Fig. 9c) than the other three samples.

Fig. 10 shows the effects of SiC particle sizes on the porosity and the flexural strength of the group P87 with 20 wt% bonding phase. It is known that the flexural strength of SiC-based porous ceramics increased with decreasing the SiC particle sizes from 300 μm to 87 μm, although the porosity of the SiC-based porous ceramics also increased from 35.5% to 42.4%. The relationship of the flexural strength to the porosity in Fig. 10 was completely contrary to the relationship given by Eq. (1). This result suggested that SiC particle sizes had much more effects on the flexural strength than the porosity, which was attributed to the fraction of the SiC particle fracture point area in the minimum solid area of fracture surface quickly increased with decreasing SiC particle sizes. The increase in the fraction of the SiC particle fracture point area in the minimum solid area of fracture surface was due to that there were more fracture points on the fracture surface of SiC-based porous ceramics composed of small SiC particles than that composed of big SiC particles. The fracture surface morphologies of SiC-based porous ceramics prepared by different sizes of SiC particles are shown in Fig. 11. It was shown that the number of the fracture points on the fracture surface increased with decreasing the SiC particle size, and the fraction of the SiC particle fracture point area in the minimum solid area of fracture surface correspondingly increased.

4. Conclusions

The effects of molding pressures, bonding phase contents, and SiC particle sizes on the flexural strength of SiC-based porous ceramics have been investigated. It is found that the flexural strength of SiC-based porous ceramics increases not only with increasing the fraction of the minimum solid area on the fracture surface, but also with increasing the fraction of the SiC particle fracture point area in the minimum solid area of fracture surface. Molding pressures of SiC-based porous ceramics affect the SiC particles stacking types, and further affect the fraction of the SiC particle fracture point area in the minimum solid area of fracture surface. The fraction of the SiC particle fracture point area in the minimum solid area of fracture surface has a peak value with increasing the bonding phase contents, and thus there is a peak value for the flexural strength of SiC-based porous ceramics. The SiC-based porous ceramic composed of small SiC particles has a bigger fraction of the SiC particle fracture point area in the minimum solid area of fracture surface than that composed of big SiC particles, and the SiC particle size has more significant effects on the flexural strength than the porosity. In a word, the proper control of molding pressures, bonding phase contents and SiC particle sizes to increase the fraction of the SiC particle fracture point area in the minimum solid area of fracture surface is the key point for preparing high strength SiC-based porous ceramics used for hot gas filter support.

Acknowledgments

The authors would like to express their gratitude for the support provided by the Ministry of Science & Technology of China (863 program, 2007AA03Z524; 973 Program, 2007CB607504), Research Fund for the Doctoral Program of Higher Education of China (20090002110010).

References

1. Lupion M, Ortiz FJG, Navarrete B, Cortes VJ. Assessment performance of high-temperature filtering elements. *Fuel* 2010;**89**:848–54.
2. Ahmadi G, Smith DH. Gas flow and particle deposition in the hot-gas filter vessel of the Pinon Pine project. *Powder Technol* 2002;**128**:1–10.
3. Mazaheri AR, Ahmadi G. Aerosol transport and deposition analysis in a demonstration-scale hot-gas filter vessel with alternate designs. *Adv Powder Technol* 2006;**17**:623–39.
4. Alvin MA. Advanced ceramic materials for use in high-temperature particulate removal systems. *Ind Eng Chem Res* 1996;**35**:3384–98.
5. Alvin MA, Lippert TE, Lane JE. Assessment of porous ceramic materials for hot gas filtration applications. *Am Ceram Soc Bull* 1991;**70**:1491–8.
6. Chi W, Jiang D, Huang Z, Tan S. Sintering behavior of porous SiC ceramics. *Ceram Int* 2004;**30**:869–74.
7. Qian JM, Jin ZH, Wang XW. Porous SiC ceramics fabricated by reactive infiltration of gaseous silicon into charcoal. *Ceram Int* 2004;**30**:947–51.
8. Zhu S, Xi HA, Li Q, Wang R. In situ growth of beta-SiC nanowires in porous SiC ceramics. *J Am Ceram Soc* 2005;**88**:2619–21.
9. Sigl LS, Kleebe HJ. Core rim structure of liquid-phase-sintered silicon carbide. *J Am Ceram Soc* 1993;**76**:773–6.
10. She JH, Ohji T, Kanzaki S. Oxidation bonding of porous silicon carbide ceramics with synergistic performance. *J Eur Ceram Soc* 2004;**24**:331–4.
11. She JH, Deng ZY, Daniel-Doni J, Ohji T. Oxidation bonding of porous silicon carbide ceramics. *J Mater Sci* 2002;**37**:3615–22.
12. She JH, Ohji T, Deng ZY. Thermal shock behavior of porous silicon carbide ceramics. *J Am Ceram Soc* 2002;**85**:2125–7.
13. Ding SQ, Zhu S, Zeng YP, Jiang DL. Effect of Y_2O_3 addition on the properties of reaction-bonded porous SiC ceramics. *Ceram Int* 2006;**32**:461–6.
14. Zhu SM, Ding SQ, Xi HA, Li Q, Wang RD. Preparation and characterization of SiC/cordierite composite porous ceramics. *Ceram Int* 2007;**33**:115–8.
15. Ding SQ, Zhu S, Zeng YP, Jiang DL. Fabrication of mullite-bonded porous silicon carbide ceramics by in situ reaction bonding. *J Eur Ceram Soc* 2007;**27**:2095–102.
16. Liu SF, Zeng YP, Jiang DL. Effects of CeO_2 addition on the properties of cordierite-bonded porous SiC ceramics. *J Eur Ceram Soc* 2009;**29**:1795–802.
17. Liu SF, Zeng YP, Jiang DL. Fabrication and characterization of cordierite-bonded porous SiC ceramics. *Ceram Int* 2009;**35**:597–602.
18. Rice RW. Evaluation and extension of physical property–porosity models based on minimum solid area. *J Mater Sci* 1996;**39**:102–18.
19. Rice RW. Evaluating porosity parameters for porosity–property relations. *J Am Ceram Soc* 2002;**76**:1801–8.
20. Rice RW. Comparison of physical property porosity behaviour with minimum solid area models. *J Mater Sci* 1996;**31**:1509–28.
21. Chae SH, Kim YW, Song IH, Kim HD, Narisawa M. Porosity control of porous silicon carbide ceramics. *J Eur Ceram Soc* 2009;**29**:2867–72.